Biosensors and Bioelectronics 143 (2019) 111604

Contents lists available at ScienceDirect

Biosensors and Bioelectronics

journal homepage: www.elsevier.com/locate/bios

Highly specific and sensitive point-of-care detection of rare circulating tumor cells in whole blood *via* a dual recognition strategy

Jianmei Yang[a], Xiaotong Huang[b], Chunfang Gan[b,*], Ruo Yuan[a], Yun Xiang[a,**]

[a] Key Laboratory of Luminescent and Real-Time Analytical Chemistry, Ministry of Education, School of Chemistry and Chemical Engineering, Southwest University, Chongqing, 400715, PR China

[b] Guangxi Key Laboratory of Natural Polymer Chemistry and Physics, Nanning Normal University, Nanning, 530001, PR China

ARTICLE INFO

Keywords:
Circulating tumor cells
Dual recognition
Glucose meter
Sensor
Signal amplification

ABSTRACT

Despite the fact that the identification and detection of circulating tumor cells (CTCs) plays a critical role in cancer monitoring and diagnosis, it remains a major challenge to isolate and detect these cells, due to their extreme scarcity in peripheral blood. In this work, by coupling a dual recognition strategy and the commercial personal glucose meter, we established a point-of-care approach for detecting rare CTCs in whole blood with high sensitivity and selectivity. The antibody-conjugated magnetic beads lead to the capture and isolation of the CTCs while the enzyme- and second antibody-modified microspheres yield the signal for detection. Because of the dual recognition format, the developed method is highly selective, and a low detection limit of 7 cells can be realized as well, owing to the great signal amplification through the enzyme-loaded microbead labels. More importantly, the detection of CTCs in whole blood can be achieved in a point-of-care fashion with the using of the glucose meter transducer, offering our method a convenient and attractive alternative to traditional biopsy for the diagnosis of various cancers.

1. Introduction

Circulating tumor cells (CTCs) are malignant cells in peripheral blood stream or lymphatic system that are shed from tumor tissues (Zhang et al., 2019; Shen et al., 2016). They play crucial roles in the occurrence of cancers and metastases (Min et al., 2015). Therefore, CTCs are considered as useful indicators of cancer metastases (Wang et al., 2019). Researches have suggested that CTCs can be found in peripheral blood during the early stages of tumorigenesis, and thus the screening of CTCs in blood can facilitate early diagnosis of different cancers, enabling the prevention of cancer metastases (Bhana et al., 2014). Moreover, CTCs contain a lot of molecular information about the primary tumors and their levels in blood are significantly associated with the progression of cancers (Lin et al., 2019; Song et al., 2017). The study on CTCs is thus of great importance for evaluating cancer dissemination, tumor stage, therapeutic responses and cancer prognosis for guiding personalized treatments (Abate et al., 2019; Chung et al., 2011; Wang et al., 2018). Compared to the gold standard of current cancer diagnosis, biopsy, CTC detection is a convenient and non-invasive “liquid biopsy” (Lv et al., 2015). However, because of the complexity of peripheral blood, the detection of CTCs suffers from two major challenges: efficient isolation and sensitive techniques available for detecting rare CTCs. The amount of CTCs in blood is extremely rare, from a few to hundreds of CTCs in 1 mL blood among about 5 billion erythrocytes and 10 million leukocytes, especially during the early stage that the primary tumor is no obvious metastasis (Yang et al., 2014; Weng et al., 2018). Because of the very low numbers of CTCs in blood, the isolation and enrichment of CTCs are necessary in CTC analyses. However, it is quite challenge to capture and separate the rare CTCs from complex blood. To overcome this obstacle, various approaches including size-based filtration (Zhang et al., 2014), density gradient sedimentation (Krivacic et al., 2004), microfluidic chip-based methods (Hyun et al., 2015), and immune-magnetic separation (Xiong et al., 2016) have been proposed to isolate and enrich the rare cancer cells from whole blood. These methods have achieved good performance in CTC isolation and enrichment. Among them, the immune-magnetic separation is the widely used strategy for CTC isolation and enrichment, owing to its high capture efficiency, fast magnetic response and easy manipulation (Wen et al., 2014). Because CTCs are commonly originated from epithelial solid tumors, which overexpress epithelial cell adhesion molecules (EpCAMs) on their surfaces, most of the currently available approaches adopted anti-EpCAM antibodies to

* Corresponding author.
** Corresponding author.
E-mail addresses: ganchunfang2008@126.com (C. Gan), yunatswu@swu.edu.cn (Y. Xiang).

https://doi.org/10.1016/j.bios.2019.111604
Received 18 June 2019; Received in revised form 6 August 2019; Accepted 15 August 2019
Available online 21 August 2019
0956-5663/

recognize and capture CTCs based on the specific interaction between anti-EpCAM antibodies and EpCAM (Viraka Nellore et al., 2015). However, CTCs may lose their epithelial nature due to the epithelial-mesenchymal transition or the tumor heterogeneity, which can lead to false negatives because the single EpCAM marker is insufficient to identify CTCs from normal cells (Chen et al., 2016). In order to improve the accuracy for CTC analyses, the combination of multiple CTC markers to capture the target cells is therefore required. In addition to the isolation and enrichment of CTCs, the detection of the captured CTCs with easy operation and high sensitivity is another challenge. Several CTC detection techniques, such as flow cytometry (FCM), immunocytochemistry (ICC), and reverse-transcriptase polymerase chain reaction (RT-PCR), have been proposed for the quantification of CTCs (Takao and Takeda, 2011; Baccelli et al., 2013; Alunni-Fabbroni and Sandri, 2010). However, these methods typically involve fluorescent staining, cell fixation, permeabilization or cell lysis, which are labor intensive and may damage the cell viability and functions (Wu et al., 2017; Xiao et al., 2017). Currently, the commercially available platform for CTC isolation and detection in the clinic is the Cell Search System, which is the only USA Food and Drug Administration (FDA) approved CTC detection method (Fang et al., 2014; Wu et al., 2016). This method requires expensive instruments and well-trained technicians. Therefore, it is urgently demanded to develop efficient and simple methods for the capture and detection of CTCs.

Personal glucose meter (PGM) is the most successfully commercialized point-of care (POC) diagnostic device used for monitoring glucose of diabetic patients, due to its simple operation, rapid response, low cost and portable pocket size (Su et al., 2013; Xiang and Lu, 2011). However, the application of the traditional PGM is limited because it can only monitor blood glucose (Su et al., 2012). To expand the applicability of PGM, several groups have developed a series of PGM-based approaches to detect a wide range of non-glucose targets, such as nucleic acids, proteins, small molecule, metal ions and enzyme activities (Zhang et al., 2016; Gu et al., 2015). In these attempts, the non-glucose targets could be quantitatively converted into glucose through the hydrolysis of sucrose by invertase, and the resulted glucose was then determined by a PGM, thus enabling the indirect detection of the target molecules. The use of PGM as the signal transduction means will therefore significantly advance the diagnosis of cancers over traditional biopsy screenings.

By following this inspiration, we propose herein a new method for the highly specific isolation and sensitive point-of-care detection of CTCs *via* the integration of the dual recognition mode, enzyme-loaded nanomaterial signal amplification labels and PGM-based readouts. The SK-BR-3 breast cancer cell line was chosen as the model target CTC. Two different antibodies, anti-EpCAM and anti-human epidermal growth factor receptor 2 (HER2) antibodies, were chosen as the recognition probes. The anti-EpCAM antibody-functionalized magnetic beads (anti-EpCAM-MBs, cMB) were used as the capture probes for CTC isolation and enrichment, and the anti-HER2 antibody and invertase co-modified polystyrene microspheres (anti-HER2/invertase-PS, sPS) were used as the signal amplification probes to convert sucrose into glucose, which was then measured by a PGM. The PGM reading could be related to the amount of glucose and further indicated the number of CTCs. The combination of multiple antibodies for targeting the cells has greatly improved the performance of the proposed strategy both in sensitivity and specificity, which enabled the simultaneous isolation and determination of CTCs in whole blood in a simple fashion.

2. Experimental section

2.1. Materials and reagents

N-(3-dimethylamminopropyl)-N′-ethylcarbodiimide hydrochloride (EDC), 2-(N-morpholino) ethanesulfonic acid (MES), Sulfo-N-hydroxysulfosuccinimide sodium salt (Sulfo-NHS), bovine serum albumin (BSA), sucrose, invertase from baker's yeast, and Dulbecco's phosphate buffered saline (DPBS) were purchased from Sigma (St. Louis, MO, USA). Carboxyl Fe_3O_4 magnetic microbeads (COOH-MB, 300–400 nm) and streptavidin-coated polystyrene microbeads (STV-PS, 500 nm) were obtained from BaseLine ChromTech Research Centre (Tianjin, China). Anti-EpCAM antibodies and biotin-labeled anti-HER2 antibodies were provided by Sino Biological Inc. (Beijing). Sulfo–NHS–LC-biotinylation kit was supplied by Pierce Biotechnology (Rockford, IL, USA). The glucose meter (Contour^{TM}TS) and test strips were provided by Bayer Healthcare LLC (Mishawaka, IN). All other reagents were of analytical grade.

2.2. Preparation of the biotin-invertase

A standard amide crosslinking method was utilized for the conjugation of the amines of invertase and NHS esters of sulfo–NHS–LC-biotin to obtain biotin-functionalized invertase (biotin-invertase). Briefly, 67 μL of 10 mM sulfo–NHS–LC-biotin was incubated with 1 mL of 5 mg mL^{-1} invertase solution for 1 h. The resulting biotin-invertase was collected after the removal of the excess biotin regent with a desalting column.

2.3. Preparation of anti-EpCAM antibody-modified MB (anti-EpCAM-MB, cMB)

The carbodiimide chemistry was utilized to covalently link amines of the anti-EpCAM antibodies with the carboxylic acid groups on the COOH-MB. Briefly, 100 μL of COOH-MB (5 mg mL^{-1}) was first washed twice with PBS buffer and then the carboxyl groups were activated by EDC (400 mM)/sulfo-NHS (100 mM) in MES buffer (0.1 M, pH 5.9) for 30 min. After three washes with PBS buffer, the activated COOH-MB was incubated with 100 μL of PBS buffer containing anti-EpCAM antibody (5 μg mL^{-1}) for 4 h at room temperature with continuous agitation. Afterward, the mixture was washed thrice with PBS solution by magnetic separation to remove unbound antibodies to obtain cMB capture probes. Finally, the resulting cMB conjugates were dispersed in 1% BSA-PBS at 5 mg mL^{-1} and stored at 4 °C for further use.

2.4. Fabrication of anti-HER2 antibody and invertase co-modified PS (anti-HER2/invertase-PS, sPS)

Biotin-anti-HER2 antibodies and biotin-invertase were conjugated to STV-PS through the interaction between streptavidin and biotin. STV-PS (100 μL, 5 mg mL^{-1}) were washed twice using PBS buffer and then mixed with 100 μL of PBS solution, which contained 5 μg mL^{-1} of biotin-anti-HER2 antibody and 0.5 mg mL^{-1} of biotin-invertase for 1 h with gentle shaking at room temperature. The resultant anti-HER2 antibody and invertase-functionalized PS (anti-HER2/invertase-PS, sPS) were washed three times using centrifugation at 8000 rpm to remove excess antibodies and invertase. Finally, the sPS were dispersed in 1% BSA-PBS at 5 mg mL^{-1} and store at 4 °C for further use.

2.5. Cell culture

The Hela cells (human cervical cancer cell line), A431 cells (human skin cancer cell line) and SK-BR-3 cells (human breast cancer cell line) were obtained from the Cell Bank of the Type Culture Collection of the Chinese Academy of Sciences (Shanghai, China). SK-BR-3 cells were cultured in RPMI-1640 medium, and A431 and Hela cells were maintained in Dulbecco's Modified Eagle Medium (DMEM). All mediums were supplemented with 1% penicillin-streptomycin and 10% fetal bovine serum (FBS). A humidified incubator with 5% CO_2 was utilized for the cell culture at 37 °C. Prior to each experiment, cells were trypsinized to detach them from the culture flask and the cell numbers were counted using a hemocytometer.

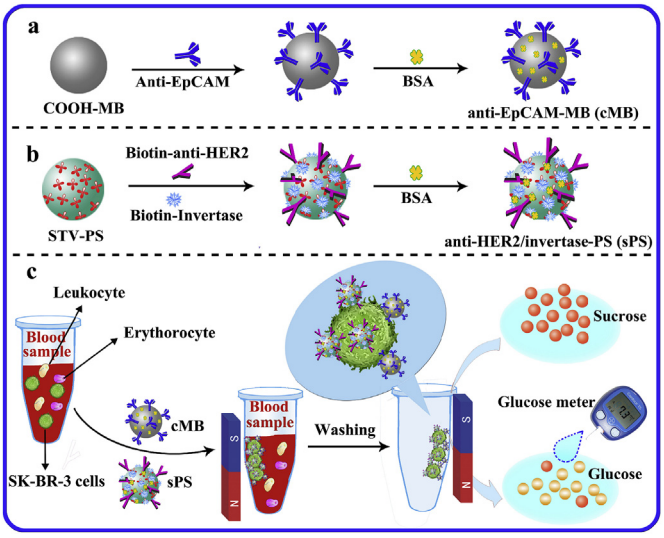

Scheme 1. Schematic illustration of specific CTC isolation and detection based on the immune-magnetic separation and the PGM transducer. The synthesis of (a) anti-EpCAM antibody-functionalized magnetic microbeads (anti-EpCAM-MBs, cMB) and (b) anti-HER2 antibody and invertase co-conjugated polystyrene microbeads (anti-HER2/invertase-PS, sPS). (c) Schematic diagram for the capture and isolation and glucometer-based determination of CTCs in whole blood.

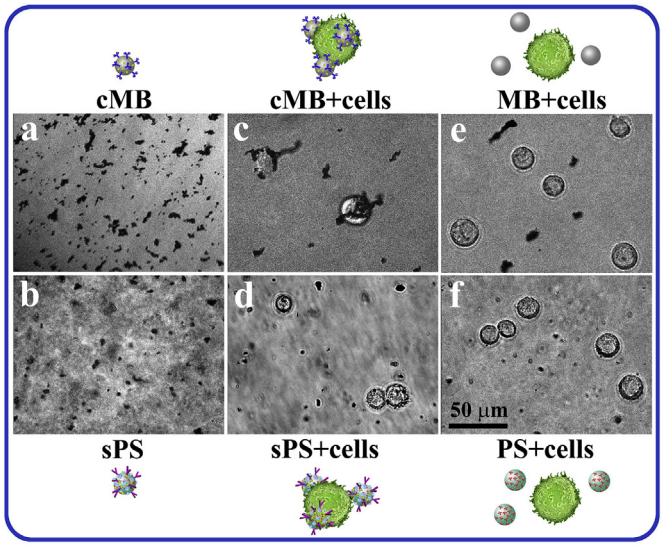

Fig. 1. Microscopy images of (a) cMB and (b) sSP; (c) cMB, (d) sPS, (e) unmodified MB and (f) unmodified PS incubated with SK-BR-3 cells.

2.6. Isolation and detection of CTCs

The probes of cMB (0.2 mg mL^{-1}, 50 μL) and sPS (0.8 mg mL^{-1}, 50 μL) were simultaneously added into 1 mL of PBS or whole blood spiked with different numbers of SK-BR-3 cells, followed by gentle stirring for 30 min at 37 °C. Then, the target CTCs were separated from the above mixture with an external magnet and washed twice using PBS buffer. The final products were further incubated with a sucrose solution (0.5 M, 100 μL) for 30 min at 37 °C, enabling the conversion of sucrose to glucose by invertase, and the generated glucose was determined by a PGM.

3. Results and discussion

3.1. CTC isolation and detection principle

Scheme 1 displays the principle of the proposed approach for CTC isolation and detection by the integration of immune-magnetic separation and PGM-based analysis. The SK-BR-3 cells were chosen as the model target CTCs. COOH-MB and STV-PS were modified with specific antibodies to capture CTCs. To improve the specificity and sensitivity of this assay, two different types of antibodies (anti-EpCAM and anti-HER2 antibodies) that can target specific proteins overexpressed on the SK-BR-3 cells were selected for the modification of COOH-MB and STV-PS. Anti-EpCAM antibodies were conjugated to COOH-MB by the amines of the anti-EpCAM antibodies *via* covalent linking to the carboxylic acid groups on COOH-MB. The obtained anti-EpCAM-MB (cMB) conjugates were used as capture probes for CTC isolation and enrichment. The STV-PS beads were functionalized with biotin-anti-HER2 antibodies and biotin-invertase through the interaction between streptavidin and biotin. The obtained anti-HER2/invertase-PS (sPS) complexes were used as signal probes for the labeling of CTCs. The target CTCs were captured by cMB and sPS through the specific interaction between the antibodies on the probes and the proteins expressed on the SK-BR-3 cells. After the separation of the target CTCs by a magnet, the captured cells were further incubated with a sucrose solution. The invertase bound to the cells could catalyze the hydrolysis of sucrose into glucose, which was further detected using a PGM. The PGM reading therefore could be related to the amount of glucose and further indicates the amount of the invertase bound to the target cells, which eventually reflected the number of the captured CTCs. In such a way, the SK-BR-3 CTCs could be successfully detected by a portable glucometer.

3.2. Validation of the interaction between SK-BR-3 cells and the probes

SK-BR-3 cells were incubated with cMB and sPS, separately, to investigate the interactions between SK-BR-3 cells and the antibodies-modified microbeads, while the unmodified microbeads (MB and PS) were used as controls. Fig. 1 shows the optical microscopic images of the probes of cMB (Fig. 1a) and sPS (Fig. 1b), and the modified and unmodified microbeads incubated with SK-BR-3 cells (Fig. 1c–f). According to Fig. 1c and d, it can be observed that the antibody-modified microbeads (cMB and sPS) are linked to the SK-BR-3 cells, which suggests that the probes can specifically recognize the target SK-BR-3 cells through the selective interaction between the antibodies and the proteins expressed on the target CTCs. In contrast, Fig. 1e and f shows that MB and PS without antibody functionalization can hardly be attached to the cell surface, indicating that the unmodified MB and PS are unable to interact with the target CTCs. All results indicate that the interactions between antibody-modified microbeads and SK-BR-3 cells are specific. Thus, the antibody-functionalized probes (cMB and sPS) could be utilized for targeting SK-BR-3 cells. Besides, the incubation of the probes with the non-specific cells (A431 cells and Hela cells) shows no noticeable interactions (Fig. S2), which further verifies the specificity of the probes for the target cells.

3.3. Feasibility of the strategy for CTC isolation and detection

To further explore the potential of the proposed strategy for the isolation and detection of CTC, the PGM readings corresponding to the SK-BR-3 cells (500 cells) incubated with different microbeads were recorded. As shown in Fig. 2a, the incubation of cMB and sPS in buffer with the absence of SK-BR-3 cells results in a very small PGM reading, which is assumably due to the nonspecific interaction between cMB and sPS. However, the PGM reading is significantly enhanced (Fig. 2b) when the SK-BR-3 cells are incubated with cMB and sPS simultaneously. This is because cMB and sPS are successfully bound to the target cells and the invertase on the sPS can convert sucrose into glucose after magnetic separation. This observation thus suggests the developed

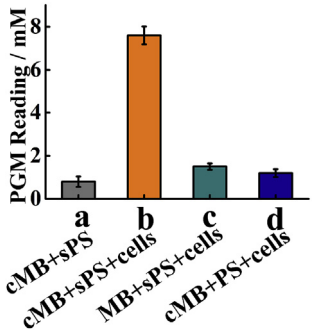

Fig. 2. PGM readings corresponding to the incubation of SK-BR-3 cells with different microbead probes with/without antibody conjugations. Error bars: SD, n = 3.

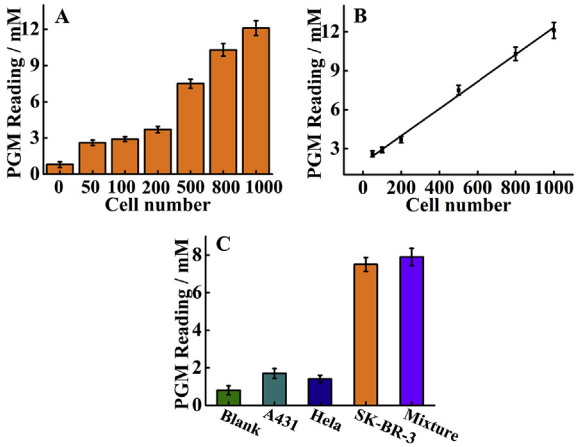

Fig. 4. Detection of SK-BR-3 cells in PBS using PGM. (A) SK-BR-3 cells with different cell numbers (0, 50, 100, 200, 500, 800 and 1000 cells) were incubated with cMB and sPS, followed by the incubation with sucrose. (B) Calibration curve of PGM reading versus SK-BR-3 cell number. (C) The PGM reading of the proposed CTC-detection method for A431 cells, Hela cells, SK-BR-3 cells, and the mixture. Error bars: SD, n = 3.

platform has great potential for the isolation and detection of CTCs. As controls, SK-BR-3 cells incubated with unmodified MB or PS were also investigated. Fig. 2c shows the PGM reading of the target CTCs incubated with unmodified MB (without anti-EpCAM antibodies) and sPS. In this case, the unmodified MBs cannot bind to the target CTCs, owing to the lack of anti-EpCAM antibodies to recognize the cells, and the cells cannot be captured after magnetic separation, resulting in small PGM reading. Similarly, an insignificant PGM reading is obtained (Fig. 2d) when the target cells are incubated with cMB and unmodified PS (without anti-HER2 antibodies) because the target CTCs are captured by cMB while almost no sPS are bound with cells due to the lack of anti-HER2 antibodies to recognize the cells. These results are consistent with the microscope imaging analyses and further demonstrate the potential of this developed strategy for the isolation and determination of CTCs.

3.4. Optimization of the experimental conditions

The sPS and cMB were employed to achieve the simultaneous isolation and detection of CTCs, in which cMB were used for separating CTCs while sPS for quantifying CTCs. Because sPS and cMB can simultaneously bind to one cell, the concentration ratio of sPS to cMB used in the CTC analysis is of great importance. Specifically, the concentration of cMB should be low enough to allow the maximum load of sPS to ensure strong PGM readings. Thus, the concentration ratio of sPS to cMB was first optimized. As shown in Fig. 3A, the PGM reading increases with increasing concentration ratio of sPS to cMB, and shows no significant change when the concentration ratio is higher than 0.8:0.2. This increase of PGM reading can be attributed to the increased amount of the sPS probes bound to the SK-BR-3 cells. However, once the concentration ratio is beyond 0.8:0.2, the attachment of sPS to SK-BR-3 cells tends to saturate. Therefore, the concentration ratio of sPS to cMB at 0.8:0.2 was chosen for the subsequent experiments. Moreover, in order to achieve the efficient and rapid capture of CTC, the incubation time of cMB and sPS with the SK-BR-3 cells was also investigated. Fig. 3B shows that the PGM reading gradually increases with the extension of incubation time from 5 to 30 min and then almost remains unchanged thereafter. Therefore, 30 min of incubation time is enough for the microbeads (cMB and sPS) to bind the target cells.

3.5. Capture and detection of SK-BR-3 cells in buffer

Under the optimal experimental conditions, the performance of the proposed approach for isolation and detection of CTC in PBS was investigated. Different numbers of SK-BR-3 cells (50, 100, 200, 500, 800 and 1000 cells) spiked in 1 mL PBS solution were incubated with cMB and sPS. After magnetic separation and incubation with sucrose, the samples were analyzed with the PGM. Fig. 4A displays the PGM readings corresponding to different numbers of SK-BR-3 cells. It can be found that the PGM reading gradually increases with the increase of the cell number. More importantly, according to Fig. 4B, we can find that the PGM reading and the cell number shows a good linear relationship in the range of 50–1000 cells with a R^2 of 0.9918. The linear equation is $Y = 0.0104X + 1.9009$ (Y is the value of PGM reading and X is the cell number). The detection limit is calculated to be 7 cells based on the 3σ rule, which is comparable or lower than previous reports (Table S1) but with a much more cost-effective and simpler way. Moreover, a relative standard deviation (RSD) of 5.6% for 500 cells (n = 6) was obtained,

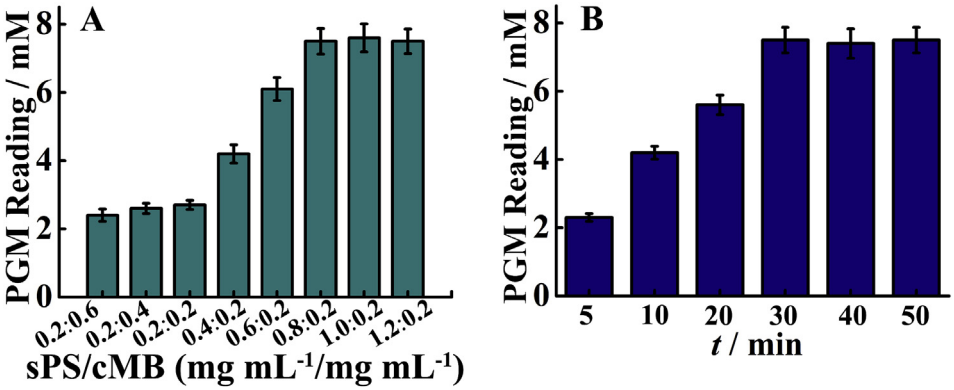

Fig. 3. Optimization of experimental conditions: (A) different concentration ratios of sPS to cMB incubated with SK-BR-3 cells, and (B) different incubation time. Error bars: SD, n = 3.

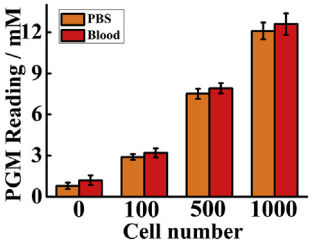

Fig. 5. PGM reading for different numbers of SK-BR-3 cells (100, 500, and 1000 cells) spiked in PBS and whole blood. Error bars: SD, n = 3.

which indicated a good reproducibility of the approach.

To investigate the specificity of the proposed CTC detection method, the A431 cells (EpCAM-positive/HER2-negative), Hela cells (EpCAM-negative), SK-BR-3 cells (EpCAM-positive/HER2-positive), and the mixture of the above cells were analyzed by this method. SK-BR-3 cells (500 cells) were used as the target CTCs while A431 and Hela cells (5000 cells) as control cells. According to Fig. 4C, the PGM readings for the A431 cells and Hela cells only have slight increases compared with the blank, while the SK-BR-3 cells with a 10-fold lower number of cells lead to an obvious increase of the PGM reading. The results suggest that our method has the specific cell recognition ability to distinguish EpCAM-positive/HER2-positive cells from other cells. Moreover, the PGM reading of the mixed cells shows a close PGM reading to that of the SK-BR-3 cells, which indicates this method has high specificity to detect the target CTCs in a large excess of negative cells. The high specificity can be attributed to the dual recognition of the cells by two different antibodies.

3.6. Capture and detection of SK-BR-3 cells in whole blood

In order to explore the potential application of the demonstrated approach to complicated samples, various amounts of SK-BR-3 cells (100, 500, and 1000 cells) were added into 1 mL whole blood to mimic CTCs in clinical blood samples, and the spiked cells were isolated and detected using the PGM method. Based on the results displayed in Fig. 5, the PGM readings for the spiked cells exhibit minor variations between whole blood and PBS, which indicates the promising application of this strategy for the isolation and determination of CTCs in real clinical samples.

4. Conclusions

In summary, an approach for highly specific and sensitive point-of-care detection of CTCs in whole blood has been demonstrated. The involvement of two distinct antibodies leads to the recognition and binding of the target CTCs with high specificity, and the use of magnetic beads and enzyme-loaded microspheres, respectively, results in effective isolation and sensitive detection of the captured CTCs. The combination of the two means together with the PGM transduction realizes point-of-care monitoring of the SK-BR-3 cells down to a few cells. Besides, the concept-of-proof verification of the method for detecting CTCs in whole blood has also been verified. These demonstrations therefore highlight the major advantages of our method for CTC detection in terms of high sensitivity (with a low detection limit of 7 cells), simplicity (point-of-care monitoring of CTCs in 1 h without complicated procedures and instruments) and applicability for real samples (detection of CTCs directly in human blood). Yet, considering the fact that CTCs may undergo epithelial to mesenchymal transition during metastasis (Lecharpentier et al., 2011), which can result in the loss of efficacy for antibody-antigen interaction, the discovery of new recognition probes, such as aptamers will significantly enhance the performance of our method in terms of specificity and versatility for simple diagnosis of different cancers.

CRediT authorship contribution statement

Jianmei Yang: Conceptualization, Data curation, Writing - original draft. **Xiaotong Huang:** Methodology, Data curation. **Chunfang Gan:** Formal analysis, Funding acquisition, Writing - review & editing. **Ruo Yuan:** Formal analysis, Writing - review & editing. **Yun Xiang:** Project administration, Conceptualization, Funding acquisition, Formal analysis, Writing - review & editing.

Declaration of competing interest

The authors declare that they have no known competing financial interests or personal relationships that could have appeared to influence the work reported in this paper.

Acknowledgment

This work was supported by National Natural Science Foundation of China (Nos. 21675128, 21762008 and 21562007) and Fundamental Research Funds for the Central Universities (XDJK2017A001).

Appendix A. Supplementary data

Supplementary data to this article can be found online at https://doi.org/10.1016/j.bios.2019.111604.

References

Abate, M.F., Jia, S.S., Ahmed, M.G., Li, X.R., Lin, L., Chen, X.Q., Zhu, Z., Yang, C.Y., 2019. Small 15 (14), 1804890.
Alunni-Fabbroni, M., Sandri, M.T., 2010. Methods 50 (4), 289–297.
Baccelli, I., Schneeweiss, A., Riethdorf, S., Stenzinger, A., Schillert, A., Vogel, V., Klein, C., Saini, M., Bäuerle, T., Wallwiener, M., Holland-Letz, T., Höfner, T., Sprick, M., Scharpff, M., Marmé, F., Sinn, H.P., Pantel, K., Weichert, W., Trumpp, A., 2013. Nat. Biotechnol. 31 (6), 539–545.
Bhana, S., Chaffin, E., Wang, Y.M., Mishra, S.R., Huang, X.H., 2014. Nanomedicine 9 (5), 593–606.
Chen, L., Wu, L.L., Zhang, Z.L., Hu, J., Tang, M., Qi, C.B., Li, N., Pang, D.W., 2016. Biosens. Bioelectron. 85, 633–640.
Chung, Y.K., Reboud, J.L., Lee, K.C., Lim, H.M., Lim, P.Y., Wang, K.Y., Tang, K.C., Ji, H.M., Chen, Y., 2011. Biosens. Bioelectron. 26 (5), 2520–2526.
Fang, S., Wang, C., Xiang, J., Cheng, L., Song, X.J., Xu, L.G., Peng, R., Liu, Z., 2014. Nano Res 7 (9), 1327–1336.
Gu, C.M., Lan, T., Shi, H.C., Lu, Y., 2015. Anal. Chem. 87 (15), 7676–7682.
Hyun, K.A., Lee, T.Y., Lee, S.H., Jung, H.I., 2015. Biosens. Bioelectron. 67, 86–92.
Krivacic, R.T., Ladanyi, A., Curry, D.N., Hsieh, H.B., Kuhn, P., Bergsrud, D.E., Kepros, J.F., Barbera, T., Ho, M.Y., Chen, L.B., Lerner, R.A., Bruce, R.H., 2004. Proc. Natl. Acad. Sci. 101 (29), 10501–10504.
Lecharpentier, A., Vielh, P., Perez-Moreno, P., Planchard, D., Soria, J.C., Farace, F., 2011. Br. J. Canc. 105 (9), 1338–1341.
Lin, Y.H., Jiang, L.L., Huang, Y.Q., Yang, Y.L., He, Y., Lu, C.H., Yang, H.H., 2019. Chem. Commun. 55 (37), 5387–5390.
Lv, S.W., Wang, J., Xie, M., Lu, N.N., Li, Z., Yan, X.W., Cai, S.L., Zhang, P.A., Dong, W.G., Huang, W.H., 2015. Chem. Sci. 6 (11), 6432–6438.
Min, H., Jo, S.M., Kim, H.S., 2015. Small 11 (21), 2536–2542.
Shen, H.W., Yang, J., Chen, Z.P., Chen, X.P., Wang, L., Hu, J., Ji, F.H., Xie, G.M., Feng, W.L., 2016. Biosens. Bioelectron. 81, 495–502.
Song, P., Ye, D.K., Zuo, X.L., Li, J., Wang, J.B., Liu, H.J., Hwang, M.T., Chao, J., Su, S., Wang, L.H., Shi, J.Y., Wang, L.H., Huang, W., Lal, R., Fan, C.H., 2017. Nano Lett. 17 (9), 5193–5198.
Su, J., Xu, J., Chen, Y., Xiang, Y., Yuan, R., Chai, Y.Q., 2012. Chem. Commun. 48 (55), 6909–6911.
Su, J., Xu, J., Chen, Y., Xiang, Y., Yuan, R., Chai, Y.Q., 2013. Biosens. Bioelectron. 45, 219–222.
Takao, M., Takeda, K., 2011. Cytometry 79A (2), 107–117.
Viraka Nellore, B.P., Kanchanapally, R., Pramanik, A., Sinha, S.S., Chavva, S.R., Hamme, A., Ray, P.C., 2015. Bioconjugate chem 26 (2), 235–242.
Wang, J., Dong, H.Y., Zhou, Y.Y., Han, L.Y., Zhang, T., Lin, M., Wang, C.H., Xu, H., Wu, Z.S., Jia, L., 2018. Biosens. Bioelectron. 122, 239–246.
Wang, S.S., Zhao, X.P., Liu, F.F., Younis, M.R., Xia, X.H., Wang, C., 2019. Anal. Chem. 91 (7), 4413–4420.
Wen, C.Y., Wu, L.L., Zhang, Z.L., Liu, Y.L., Wei, S.Z., Hu, J., Tang, M., Sun, E.Z., Gong, Y.P., Yu, J., Pang, D.W., 2014. ACS Nano 8 (1), 941–949.
Weng, W.H., Ho, I.L., Pang, C.C., Pang, S.N., Pan, T.M., Leung, W.H., 2018. Biosens. Bioelectron. 116, 51–59.
Wu, J., Wei, X., Gan, J.R., Huang, L., Shen, T., Lou, J.T., Liu, B.H., Zhang, J.X.J., Qian, K., 2016. Adv. Funct. Mater. 26 (22), 4016–4025.

Wu, L.L., Wen, C.Y., Hu, J., Tang, M., Qi, C.B., Li, N., Liu, C., Chen, L., Pang, D.W., Zhang, Z.L., 2017. Biosens. Bioelectron. 94, 219–226.
Xiang, Y., Lu, Y., 2011. Nat. Chem. 3 (9), 697–703.
Xiao, L., He, Z.B., Cai, B., Rao, L., Cheng, L., Liu, W., Guo, S.S., Zhao, X.Z., 2017. Chem. Phys. Lett. 668, 35–41.
Xiong, K., Wei, W., Jin, Y.J., Wang, S.M., Zhao, D.X., Wang, S., Gao, X.Y., Qiao, C.M., Yue, H., Ma, G.H., Xie, H.Y., 2016. Adv. Mater. 28 (36), 7929–7935.
Yang, H.W., Lin, C.W., Hua, M.Y., Liao, S.S., Chen, Y.T., Chen, H.C., Weng, W.H., Chuang, C.K., Pang, S.T., Ma, C.C.M., 2014. Adv. Mater. 26 (22), 3662–3666.
Zhang, H.Y., Wang, Y.H., Li, Q.L., Zhang, F.M., Tang, B., 2014. Chem. Commun. 50 (53), 7024–7027.
Zhang, J.J., Xiang, Y., Wang, M., Basu, A., Lu, Y., 2016. Angew. Chem. Int. Ed. 55 (2), 732–736.
Zhang, Q.W., Ouyang, J., Wang, Y., Zhai, T.T., Wang, C., Wu, Z.Q., Zhang, T.Q., Wang, K., Xia, X.H., 2019. Biosens. Bioelectron. 138, 111316.